



HAL
open science

Late Lutetian Thermal Maximum-Crossing a Thermal Threshold in Earth's Climate System?

T. Westerhold, U. Röhl, B. Donner, T. Frederichs, W. Kordesch, S. Bohaty,
D. Hodell, J. Laskar, R. Zeebe

► **To cite this version:**

T. Westerhold, U. Röhl, B. Donner, T. Frederichs, W. Kordesch, et al.. Late Lutetian Thermal Maximum-Crossing a Thermal Threshold in Earth's Climate System?. *Geochemistry, Geophysics, Geosystems*, 2018, 19 (1), pp.73-82. 10.1002/2017GC007240 . hal-02318056

HAL Id: hal-02318056

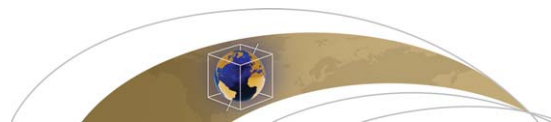
<https://hal.science/hal-02318056>

Submitted on 20 Dec 2021

HAL is a multi-disciplinary open access archive for the deposit and dissemination of scientific research documents, whether they are published or not. The documents may come from teaching and research institutions in France or abroad, or from public or private research centers.

L'archive ouverte pluridisciplinaire **HAL**, est destinée au dépôt et à la diffusion de documents scientifiques de niveau recherche, publiés ou non, émanant des établissements d'enseignement et de recherche français ou étrangers, des laboratoires publics ou privés.

Copyright



RESEARCH ARTICLE

10.1002/2017GC007240

Late Lutetian Thermal Maximum—Crossing a Thermal Threshold in Earth's Climate System?

Key Points:

- Eocene transient (30 kyr) warming event at 41.52 Ma
- The Late Lutetian Thermal Maximum (LLTM) occurs within magnetochron C19r and is characterized by a $\sim 2^{\circ}\text{C}$ warming of the deep ocean in the southern South Atlantic
- LLTM coincides with exceptionally high insolation pointing to a potential thermal threshold of Earth's climate system

Supporting Information:

- Supporting Information S1

Correspondence to:

T. Westerhold,
twesterhold@marum.de

Citation:

Westerhold, T., Röhl, U., Donner, B., Frederichs, T., Kordesch, W. E. C., Bohaty, S. M., . . . Zeebe, R. E. (2018). Late Lutetian Thermal Maximum—Crossing a thermal threshold in Earth's climate system? *Geochemistry, Geophysics, Geosystems*, 19, 73–82. <https://doi.org/10.1002/2017GC007240>

Received 15 SEP 2017

Accepted 17 DEC 2017

Accepted article online 27 DEC 2017

Published online 12 JAN 2018

T. Westerhold¹ , U. Röhl¹ , B. Donner¹, T. Frederichs² , W. E. C. Kordesch³, S. M. Bohaty³ , D. A. Hodell⁴ , J. Laskar⁵, and R. E. Zeebe⁶ 

¹MARUM – Center for Marine Environmental Sciences, University of Bremen, Bremen, Germany, ²Faculty of Geosciences, University of Bremen, Bremen, Germany, ³Ocean and Earth Science, University of Southampton, Waterfront Campus, National Oceanography Centre, Southampton, UK, ⁴Godwin Laboratory for Palaeoclimate Research, Department of Earth Sciences, University of Cambridge, Cambridge, UK, ⁵Astronomie et Systèmes Dynamiques, IMCCE-CNRS UMR8028, Observatoire de Paris, UPMC, Paris, France, ⁶School of Ocean and Earth Science and Technology, University of Hawai'i at Manoa, Honolulu, HI, USA

Abstract Recognizing and deciphering transient global warming events triggered by massive release of carbon into Earth's ocean-atmosphere climate system in the past are important for understanding climate under elevated pCO₂ conditions. Here we present new high-resolution geochemical records including benthic foraminiferal stable isotope data with clear evidence of a short-lived (30 kyr) warming event at 41.52 Ma. The event occurs in the late Lutetian within magnetochron C19r and is characterized by a $\sim 2^{\circ}\text{C}$ warming of the deep ocean in the southern South Atlantic. The magnitudes of the carbon and oxygen isotope excursions of the Late Lutetian Thermal Maximum are comparable to the H2 event (53.6 Ma) suggesting a similar response of the climate system to carbon cycle perturbations even in an already relatively cooler climate several million years after the Early Eocene Climate Optimum. Coincidence of the event with exceptionally high insolation values in the Northern Hemisphere at 41.52 Ma might indicate that Earth's climate system has a thermal threshold. When this tipping point is crossed, rapid positive feedback mechanisms potentially trigger transient global warming. The orbital configuration in this case could have caused prolonged warm and dry season leading to a massive release of terrestrial carbon into the ocean-atmosphere system initiating environmental change.

1. Introduction

The warm world in and around the Early Eocene Climate Optimum (EECO; 53–50 Ma) was punctuated by transient global warming events (hyperthermals) of various magnitude (Kirtland Turner et al., 2014) (Figure 1). These events provide important insight into the complex interaction and feedback mechanism operating under greenhouse conditions (Dickens, 2003; Kirtland Turner et al., 2014; Lunt et al., 2011; Zachos et al., 2008). In deep-marine sediments, hyperthermal events can be identified by a paired negative excursion in the carbon and oxygen isotope composition of bulk sediment and benthic foraminifera, associated with a more clay-rich layer indicating dissolution of carbonate (Leon-Rodriguez & Dickens, 2010; Lourens et al., 2005; Zachos et al., 2005). Except for the Paleocene/Eocene Thermal Maximum, which is by far the most pronounced Eocene hyperthermal event, all Cenozoic hyperthermals are shown to be paced by Earth's orbital eccentricity (Cramer et al., 2003; Lauretano et al., 2015, 2016; Sexton et al., 2011; Zachos et al., 2010).

In deep-sea sediment cores younger than 47 Ma, there is limited evidence for additional hyperthermal events caused by a transient release of carbon from any exchangeable carbon reservoir. Variations in insolation might not have reached the thermodynamic threshold to release gas hydrates or cause significant changes in ocean ventilation after global temperature had cooled sufficiently after the EECO (Kirtland Turner et al., 2014) or the gas hydrate (storage) capacity was no longer sufficient (Nicolo et al., 2007). However, at ODP Site 1260 on Demerara Rise in the equatorial Atlantic, a hyperthermal event has been identified that occurred almost 10 million years after the EECO (Leg 207; Erbacher et al., 2004). This event, dated at 41.520 Ma (Westerhold & Röhl, 2013), was named the “C19r event” after its location in magnetochron C19r (C19r.72) (Edgar et al., 2007) (Figure 1). Because the C19r hyperthermal event is located in the late Lutetian in the middle Eocene, we refer to it as the Late Lutetian Thermal Maximum (LLTM) hereafter. The intense

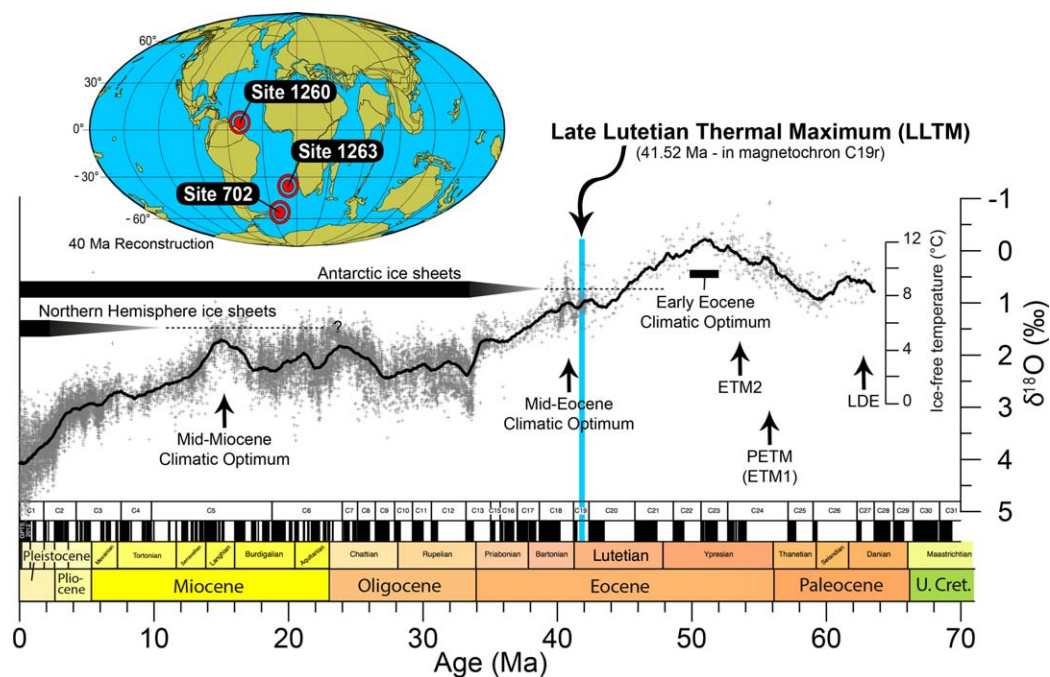


Figure 1. Overview of the position of the LLTM within the Cenozoic climate evolution represented by the deep-sea benthic stable oxygen isotope reference curve (modified after Zachos et al., 2001). Location map for ODP Sites 702, 1260, and 1263 on a 40 Ma paleogeographic reconstruction in Mollweide projection (from <http://www.ods.n.de>) that have been studied to investigate the magnitude of the LLTM. Position of prominent Eocene and Paleocene global warming events are shown: LDE, Latest Danian Event; PETM, Paleocene/Eocene Thermal Maximum, aka ETM1; ETM-2, Eocene Thermal Maximum 2.

dissolution of carbonate at Site 1260 across this event, with CaCO_3 concentrations decreasing from 75 to 35% (Edgar et al., 2007), has prevented the development of benthic stable isotope records at this site, which would allow assessment of the magnitude of the deep water carbon isotope excursion (CIE) and warming.

Up to now, the full magnitude of the LLTM and its global relevance have not been adequately characterized. The LLTM is of special interest because it coincides with the highest insolation value (573 W m^{-2}) of the last 45 Ma using the La2004 solution at 65°N on 21 June (Laskar et al., 2004; Westerhold & Röhl, 2013). Notably, an insolation value of $\sim 560 \text{ W m}^{-2}$ was reached about 400 kyr prior to the LLTM, but no CIE, no oxygen isotope record indicating warming or peculiar Fe intensity peak points to a hyperthermal event at that time. The additional 13 W m^{-2} may have triggered a hyperthermal event. It would be of great interest for modeling studies to know the magnitude of the carbon and oxygen isotope excursion in the deep sea during the LLTM. The transient nature of the event makes it difficult to identify the LLTM in deep-sea sediments without high resolution (hundreds) of stable isotope analysis, but because of its position 72% up in magnetic polarity reversal chron C19r it should be feasible to locate the LLTM if a reliable magnetostratigraphy is available.

Here we present X-ray fluorescence (XRF) core scanning Fe intensities, magnetic properties, core images, coulometrically determined carbonate content, and stable carbon and oxygen isotope data (bulk, benthic and planktic foraminifera) from ODP Sites 702 and 1263 showing that the LLTM is a transient hyperthermal event.

2. Materials, Methods, and Age Model

Site 702 ($50^\circ 56.760'S$, $26^\circ 22.122'W$; Shipboard Scientific Party, 1988) is located near the crest of the Islas Orcadas Rise in the southern South Atlantic in 3,083 m water depth, $\sim 2,200$ m water depth in middle Eocene. ODP Site 1263 ($28^\circ 31.977'S$, $2^\circ 46.774'E$) is located on the Walvis Ridge in the SE Atlantic (Zachos et al., 2004) in 2,717 m water depth, $\sim 1,900$ m water depth in middle Eocene. The event was initially

identified by careful analysis of magnetostratigraphy and XRF scanning data. Subsequently stable isotope data from bulk, benthic and planktic foraminifera as well as coulometric CaCO_3 wt% were generated and helped to refine the details of the event. The new records are integrated with the astronomical age model of ODP Site 1260 and compared to published key records (Bohaty et al., 2009; Edgar et al., 2007; Westerhold & Röhl, 2013). Details of the methods, additional tables and data are available in the supporting information and open access online at <https://doi.pangaea.de/10.1594/PANGAEA.883619>.

A high-resolution age model based on astronomical tuning of eccentricity-modulated precession cycles in XRF Fe intensity data is available for Site 1260 (Westerhold & Röhl, 2013). For Hole 702B and Site 1263, a 405 kyr age model exists below 121.26 mbsf and 175.41 rmcd, respectively (Westerhold et al., 2015). To both refine and extend these existing age models for Hole 702B and Site 1263, the bulk $\delta^{13}\text{C}$ and Fe intensity data on depth scale have been correlated to the benthic $\delta^{13}\text{C}$ and Fe data of Site 1260 (supporting information Figures S6 and S7). The Fe peak of the LLTM was dated to 41.520 Ma (Westerhold & Röhl, 2013) and used as correlation horizon between the sites. The resulting age models for Hole 702B, Site 1260, and Site 1263 are provided in supporting information Table S12.

3. Results

New magnetostratigraphic and XRF core scanning data help to find the LLTM as recorded in deep-sea drilling sites (Figure 2). At Site 1260, the LLTM is characterized by strong dissolution expressed in a dark, clay-rich layer and a distinct peak in XRF scanning Fe intensities as well as by a negative CIE of 0.86‰ in bulk sediment and 1.26‰ in the planktic foraminiferal species *M. lehnerei* (Edgar et al., 2007; Westerhold & Röhl, 2013). New data from Hole 702B (Figure 3) reveal a pronounced peak in Fe intensity, a slight decrease in carbonate content from 91 to 78%, a 0.55‰ decrease in bulk carbonate $\delta^{13}\text{C}$, a 1.27‰ decrease in planktic foraminiferal $\delta^{13}\text{C}$, and a 0.77‰ decrease in benthic foraminiferal $\delta^{13}\text{C}$. At Site 1263, a slight decrease in carbonate content from 93 to 83% can be observed in addition to a 0.34‰ decrease in bulk sediment $\delta^{13}\text{C}$ and a maximum decrease of 1.23‰ in benthic foraminiferal $\delta^{13}\text{C}$ (Figure 3). Sites 702 and 1263 also show a consistent decrease in benthic oxygen isotope data of 0.48‰ (702) and 0.53‰ (1263) during the event, and planktic foraminifera from Hole 702B exhibit also a decrease of 0.41‰ in $\delta^{18}\text{O}$ (supporting information). Bulk carbonate $\delta^{18}\text{O}$ data show only a minor excursion at Hole 702B and no excursion at Site 1263. The pattern in bulk $\delta^{13}\text{C}$ as well as planktic and benthic stable isotope data are characteristic of a transient hyperthermal event with a rapid shift at the onset, an interval with lower carbonate content and high Fe intensities in the more clay-rich layer after the onset, a period of lighter $\delta^{13}\text{C}$ isotope values in the center of the event and a final recovery to background levels. The magnitude of the CIE for the LLTM based on data from all three sites is $\sim 0.8\text{‰}$ on average, and the event is associated with a warming of $\sim 2^\circ\text{C}$ estimated from the 0.5‰ decrease in $\delta^{18}\text{O}$ (paleotemperature after Erez & Luz, 1983; -1.2‰ ice-free SMOW).

4. Discussion

4.1. Duration of the LLTM

The duration of the event was first estimated to be in the order of 40–50 kyr, similar to other transient hyperthermals in the early to middle Eocene (Westerhold & Röhl, 2013). Application of the new astronomical age model suggests that the duration of the LLTM CIE—from onset to recovery to background levels in $\delta^{13}\text{C}$ —spans only 30 kyr. The clay layer of maximum carbonate dissolution is only 5 kyr and carbonate content was lowered with respect to the average normal concentration for 15 kyr. The onset of the CIE to the peak warming of 2°C took about 7 kyr (Figure 4), and the warming lasted ~ 10 kyr.

To test the astronomical duration estimates of the above mentioned features, durations can be alternatively estimated from average sedimentation rates calculated using the Cande and Kent (1995) and GPTS 2012 (Vandenberghe et al., 2012) time scale datums for magnetic polarity chron C19r. Sedimentation rates are in the order of 1.20–1.34 cm kyr^{-1} for Hole 702B, 2.08–2.32 cm kyr^{-1} for Site 1260, and 0.78–0.87 cm kyr^{-1} for Site 1263. The LLTM CIE at Hole 702B is about 45 cm or 10.42–11.61 kyr applying the Cande and Kent (1995) and the GPTS 2012 (Vandenberghe et al., 2012) estimates for the duration of chron C19r. The clay layer has a thickness of 7 cm at Hole 702B and 9 cm at Site 1260, which translates into durations of 5.32–5.82 and 3.88–4.32 kyr, respectively. Carbonate content at Site 1260 was lower for about 28 cm or 12.06–13.44 kyr.

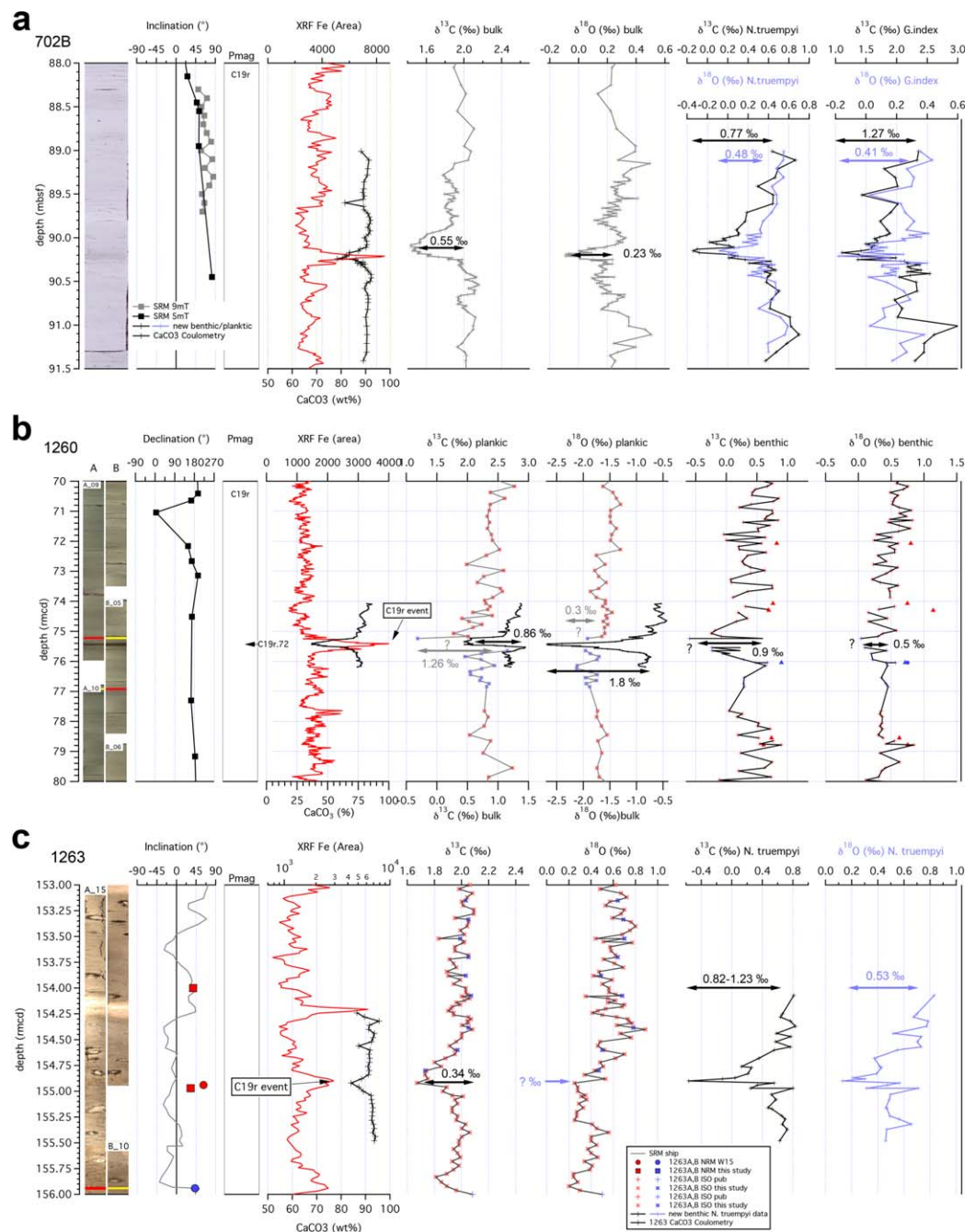


Figure 2. Close up overview of data covering the LLTM interval of (a) Hole 702B, (b) Site 1260, and (c) Site 1263. From left to right: core images, inclination (Clement & Hailwood, 1991; Edgar et al., 2007; Ogg & Bardot, 2001; Westerhold et al., 2015; Zachos et al., 2004; this study), magnetostratigraphic interpretation, XRF core scanning Fe intensities (Westerhold & Röhl, 2013; Westerhold et al., 2015; this study), coulometric CaCO₃ content (this study), bulk sediment carbon and oxygen isotope values (Bohaty et al., 2009; Westerhold et al., 2015; this study), and benthic and planktic foraminifer carbon and oxygen isotope values (Edgar et al., 2007; Katz & Miller, 1991; Sexton et al., 2006; this study). Position of LLTM at C19r.72.

Results from this simple calculation reveal even slightly shorter durations for the prominent features of the LLTM, but essentially support the astronomical age model established here.

The magnitudes of the CIE and $\delta^{18}\text{O}$ excursion are comparable to the H2 event (53.95 Ma age from Westerhold et al., 2017; Stap et al., 2010; Laurentano et al., 2016; see supporting information Figure S8) and to the numerous hyperthermal events in early to middle Eocene (50–48 Ma; Sexton et al., 2011), suggesting a

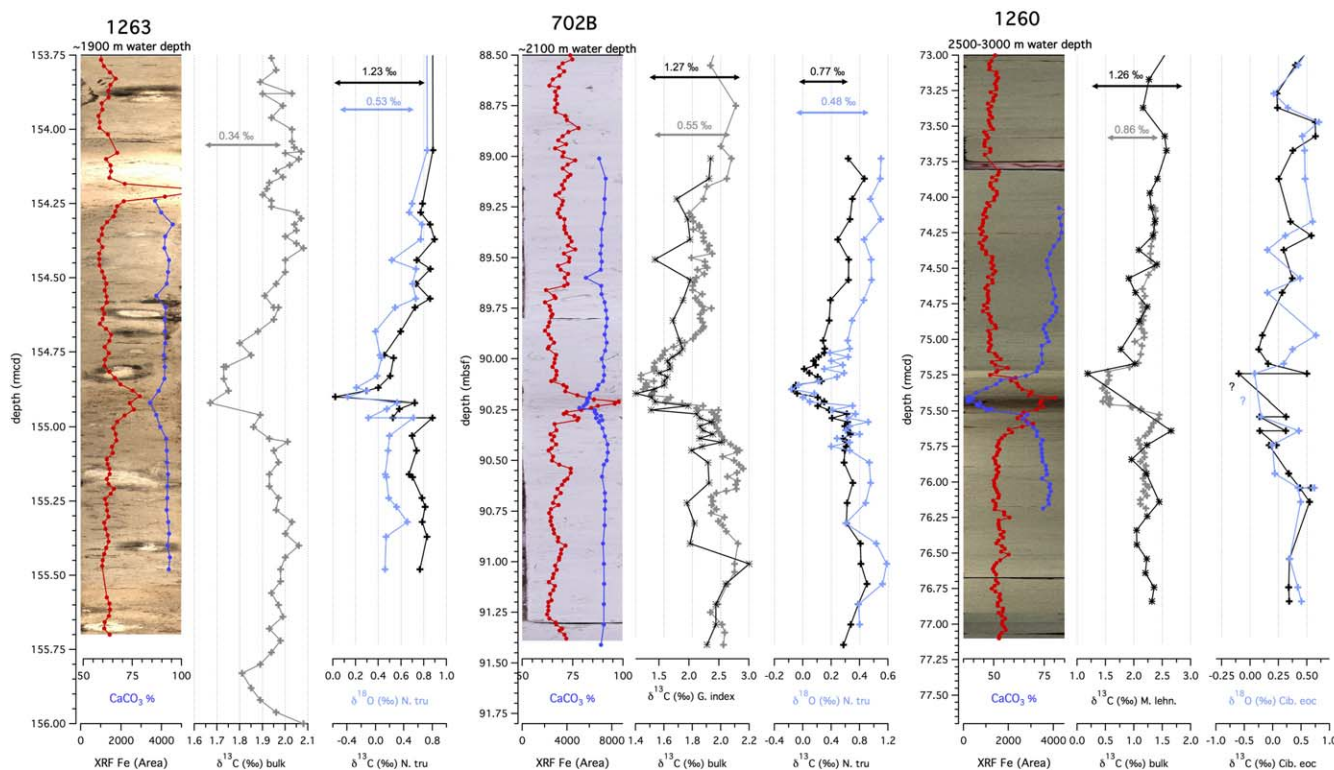


Figure 3. Core images and geochemical data across the Late Lutetian Hyperthermal Maximum layer for ODP Site 1263, Hole 702B, and Site 1260 plotted versus depth. The event is indicated by a Fe intensity peak (red line with dots), a decrease in CaCO₃ content (blue line with dots), a bulk δ¹³C (gray line with crosses), benthic foraminifera δ¹³C (black line with crosses), and δ¹⁸O (blue line with crosses) anomaly in all records. This anomaly is also observed in planktic foraminifera δ¹³C (black line with stars) in Hole 702B and at Site 1260. Arrows indicate the excursion size. Water depth are backtracked paleo-water depth (Site 1260 data from Edgar et al., 2007; Westerhold & Röhl, 2013).

similar response of the climate system to carbon cycle perturbations even in the relatively cooler climate state of the late middle Eocene. The Latest Danian Event (LDE; Bornemann et al., 2009) occurred more than 20 million years before the LLTM, but in a very similar absolute temperature background with respect to deep-sea temperatures (see Figure 1). LLTM and LDE have the transient onset of the CIE and an overall 2°C increase in deep-sea temperatures in common. But the LDE is characterized by a double peak in stable carbon isotope data with a total duration of 200 kyr (Westerhold et al., 2011), much longer than the 30 kyr of the LLTM CIE. Interestingly, the duration of the LLTM is comparable to the H2 event which occurred under warmer climate conditions just prior to the EECO (Figure 1). Despite the difference in absolute temperature background with respect to deep-sea temperatures the LLTM seems to be more comparable in magnitude and duration to the early Eocene H2 event than to the LDE.

4.2. Looking for Causal Mechanism—A First Approach

The LLTM exhibits all typical patterns of hyperthermal events but is asymmetric because of its abrupt onset, was shorter than known Eocene warming events, and shows clear evidence of an extraordinary orbital trigger (Westerhold & Röhl, 2013). The ~7 kyr delay from the onset of the warming event, marked by the inception of the carbonate content, to peak δ¹⁸O values suggests that most of the recorded warming occurred after the release of carbon which increased atmospheric pCO₂ and led to greenhouse warming. Enhanced dissolution of carbonate with increasing paleo-depth can be observed at the three sites, which we interpret as related to a transient shoaling of the carbonate compensation depth (CCD). During the middle Eocene the CCD in the Atlantic was much shallower (~3,500 m at Walvis Ridge) than today (Van Andel, 1975; Zachos et al., 2004). No significant CCD changes have been observed one million years before and after the event as expressed by regular Fe cyclicity in the Site 1260 record (Westerhold & Röhl, 2013). The observed drop from 75 to 35% calcium carbonate at Site 1260 (~2,500 m paleo-water depth) during the LLTM indicates that the CCD shoaled by 500–1,000 m for about 5 kyr. Modeling of the carbonate chemistry of surface

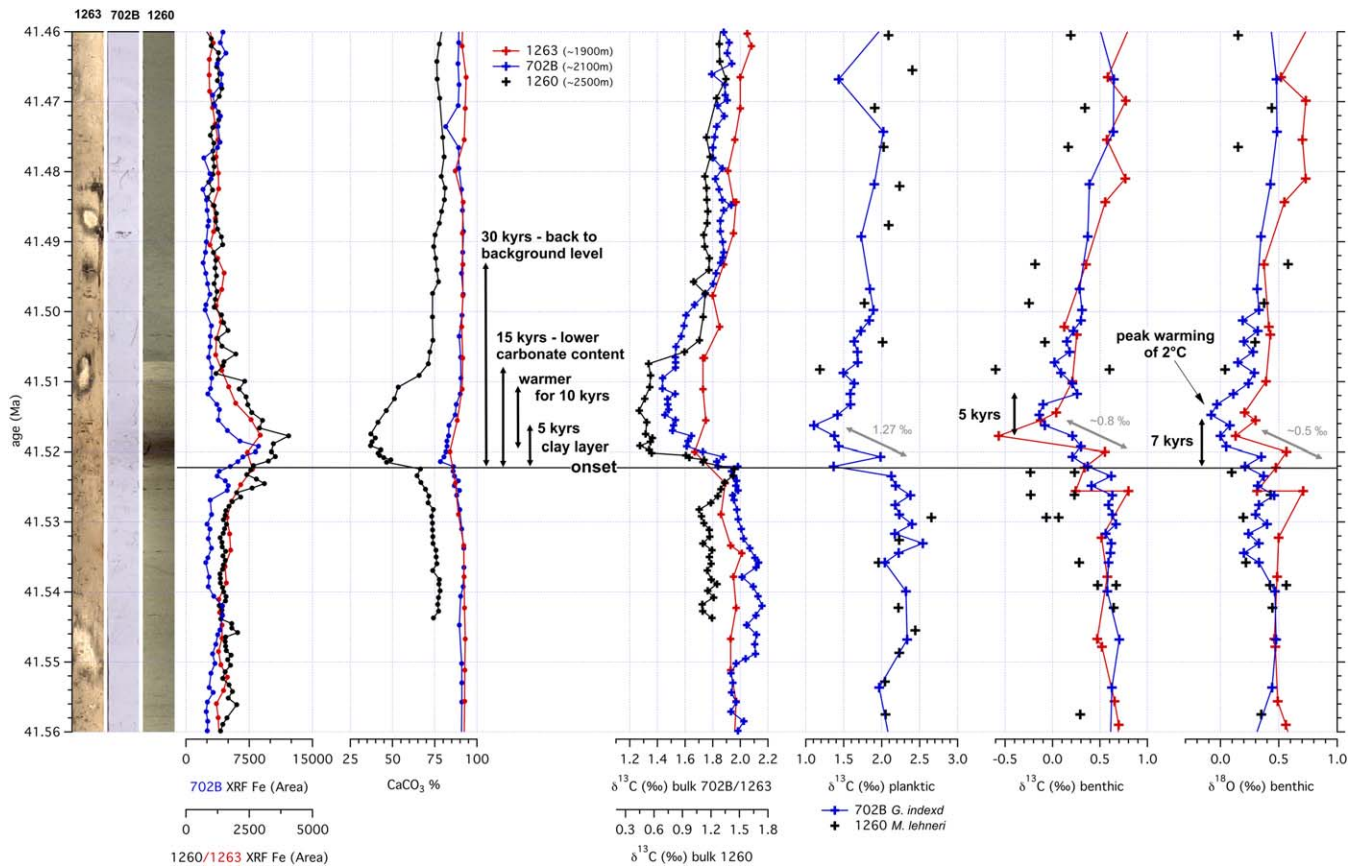


Figure 4. Core images and geochemical data across the LLTM for ODP Site 1263 (red), Hole 702B (blue), and Site 1260 (black) plotted versus age. Shoaling of the CCD during the event could explain the greater decrease in carbonate content with depth. According to our age model, warming lasted for about 10 kyr with peak values reached ~7 kyr after the onset. It took about 30 kyr for the bulk $\delta^{13}\text{C}$ data in Hole 702B to return to preexcursion values.

and deep waters under late Paleocene boundary conditions shows that a uniform ~2,000 Pg release of carbon to the atmosphere over 1 kyr (Ridgwell & Schmidt, 2010) could cause a CCD rise as observed at the LLTM. A release of ~1,000 Pg of carbon from oxidation of terrestrial/marine organic matter would also be enough to cause a ~1‰ CIE (Pagani et al., 2006) during the LLTM. As proposed for multiple Eocene hyperthermal events (Sexton et al., 2011) the LLTM could have been caused alternatively by large-scale releases of dissolved organic carbon from the ocean by ventilation of the ocean interior. The rapid recovery of the carbon isotope data to background levels also suggests that carbon was quickly resequenced by the ocean and on land, rather than removed by silicate rock weathering (Sexton et al., 2011; Penman et al., 2016).

For a better understanding of the observations, we ran two simple carbon cycle model scenarios (Figure 5 and Table 1) with the Long-term Ocean-atmosphere-Sediment Carbon cycle Reservoir Model (LOSCAR; Zeebe, 2012). The first scenario uses carbon input from a methane source, while the second scenario uses organic carbon input (Corg) with parameters as given in Table 1 in order to replicate the observed CIE and Atlantic %CaCO₃ drop during the LLTM. To be consistent with the latter observation, the methane scenario (with slightly lower emissions) requires ~40% of the carbon to be input directly into the deep Atlantic. In addition, the methane scenario would need a higher climate sensitivity/Earth System Sensitivity (ESS) than the Corg scenario to produce a similar surface warming. The initial, steady state atmospheric CO₂ concentration of 750 ppmv was selected based on recent CO₂ estimates at ~40 Ma using boron isotopes (Anagnostou et al., 2016). Two interesting observations can be made: (1) The surface warming is only ~1.2 K in both runs, less than the estimated 2 K from the benthic stable isotope data. This is perhaps not too surprising if the carbon did not cause all the warming. In fact, for the methane scenario, some initial warming would be required to trigger methane clathrate destabilizing at the seafloor. Unusual warming could be related to

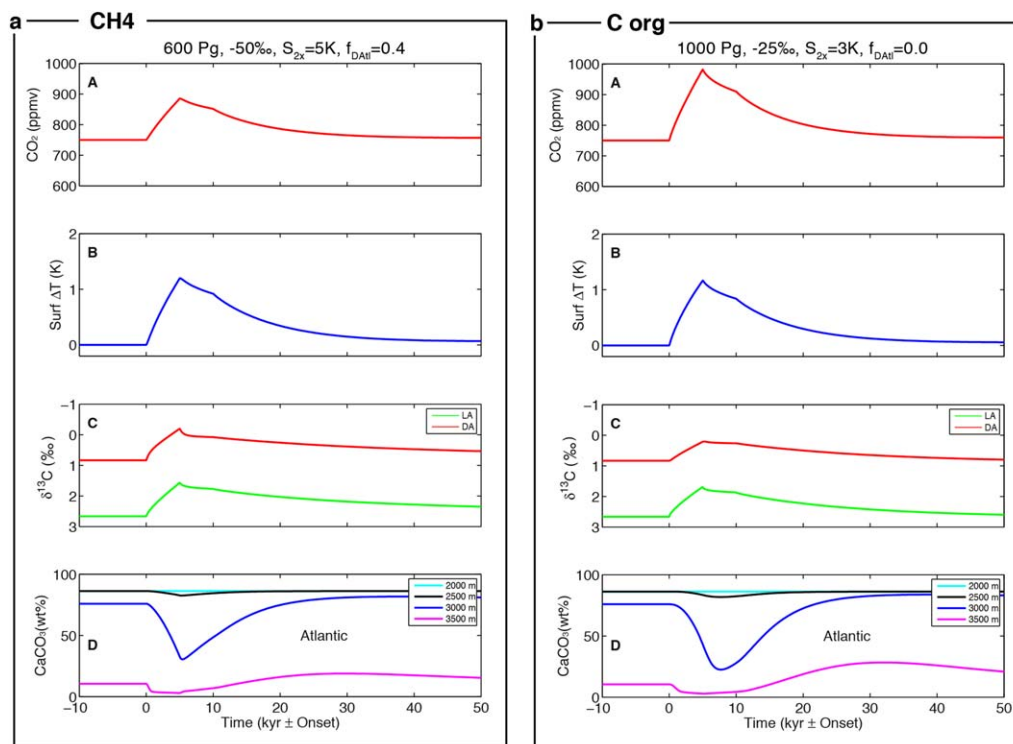


Figure 5. Two LOSCAR model run outputs for (a) a carbon input scenario based on a methane source (rapidly oxidized to CO_2) and (b) a Corg input with parameters as given in Table 1 to replicate the observed CIE and Atlantic CaCO_3 drop during the LLTM. S_{2x} is climate sensitivity/ESS and f_{DAtl} is the C fraction released into the deep Atlantic. (A) Simulated atmospheric CO_2 for each carbon-release scenario, (B) simulated surface temperature increase, (C) simulated $\delta^{13}\text{C}$ of TCO_2 in the low-latitude surface Atlantic (LA) and deep Atlantic Ocean (DA), and (D) simulated wt% CaCO_3 at various depths in the deep Atlantic.

exceptionally high insolation. (2) The model recovery, particularly $\delta^{13}\text{C}$, is slower than observed. Therefore, some sequestration of organic carbon during recovery (Figure 5, starting at 10 kyr, see kinks in graphs) at 20% of the input rate and then dropping exponentially was included in the model. Both model runs show that to some extent the injection of 600–1,000 Pg of carbon could explain the observed CIE and dissolution of carbonate at the Atlantic ODP sites. However, both scenarios unfortunately say little about the potential threshold behavior with respect to orbital forcing. Other models like the Kirtland Turner et al. (2014) model are conceptual models that will also not predict realistic threshold behavior. Ultimately, this may require a fully coupled carbon cycle-climate model and a comprehensive understanding (and implementation) of various insolation effects on (and feedbacks between) the climate system and the carbon cycle. Even if such a model existed today, it is unknown whether it would exhibit a threshold behavior that explains the LLTM observations.

Compared to the early Eocene hyperthermals, the middle Eocene LLTM shows a similar relationship between the phasing and amplitude of $\delta^{13}\text{C}$ and $\delta^{18}\text{O}$ excursions (Figure 6). For early Eocene events, a decrease of 1‰

in benthic $\delta^{13}\text{C}$ is associated with a 0.6‰ decrease in $\delta^{18}\text{O}$ (Lauretano et al., 2015; Stap et al., 2010). Similarly for the LLTM, a decrease of 1‰ in benthic $\delta^{13}\text{C}$ is associated with a 0.5‰ decrease in $\delta^{18}\text{O}$ suggesting a slightly weaker climate sensitivity (PALAEOSENS Project Members, 2012) or a different carbon source (through variable greenhouse effects; Dickens, 2011). The exceptionally strong insolation in the orbital solution at 41.52 Ma may indeed have been responsible for crossing a threshold leading to the rapid release of carbon into the ocean-atmosphere system causing the LLTM (Westerhold & Röhl, 2013).

Exceptionally high insolation at 65°N on 21 June is a result of the alignment of maximum obliquity with a high eccentricity-modulated

Table 1

Input Parameters for the LOSCAR Simple Carbon Cycle Model Scenarios where S_{2x} is Climate Sensitivity/ESS and f_{DAtl} is the C Fraction Released Into the Deep Atlantic (Zero for Corg Input)^a

	C input (Pg C)	$\delta^{13}\text{C}$ (‰)	S_{2x} (K)	f_{DAtl}
CH ₄	600	−50	5.0	0.4
Corg	1,000	−25	3.0	0.0

^a $\delta^{13}\text{C}_s = \delta^{13}\text{C}$ of source carbon. The methane scenario assumes rapid oxidation of CH_4 to CO_2 . For results see Figure 5.

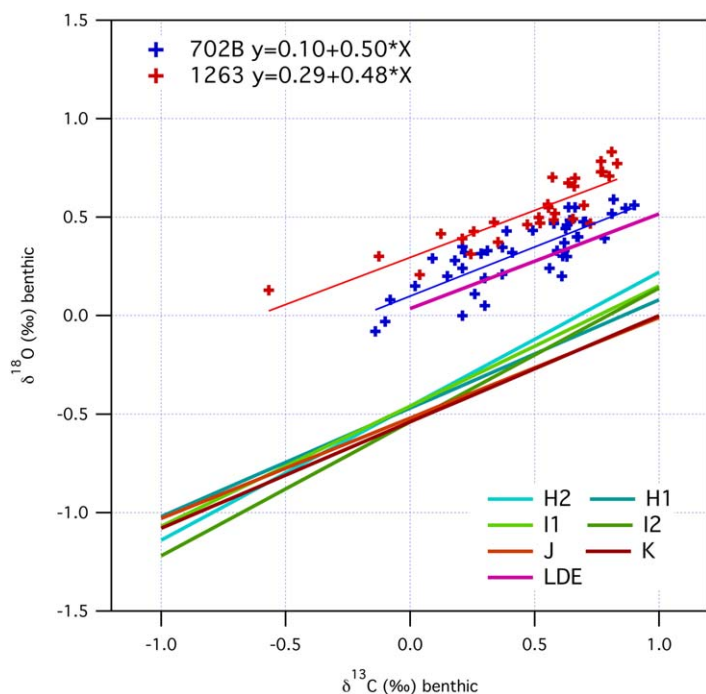


Figure 6. Oxygen versus carbon isotope data (*N. truempyi*) for samples from the LLTM in Hole 702B (blue crosses) and at Site 1263 (red crosses). For comparison, the linear regression lines for the LDE (Westerhold et al., 2011) and early Eocene hyperthermal events H1, H2, I1, I2, J, and K for Site 1263 data are shown (Lauretano et al., 2015; Stap et al., 2010; the H1 line is from Site 1265). This demonstrates that the changes during the LLTM are linearly related to warming with a similar slope for $\delta^{18}\text{O}$ to $\delta^{13}\text{C}$ changes as observed for early Eocene hyperthermal events at Walvis Ridge. Due to the $\sim 3^\circ\text{C}$ cooler climate (Zachos et al., 2008), the regression for the $\delta^{18}\text{O}$ LLTM is offset by $+0.75\text{‰}$ compared to the early Eocene events, plotting close to the regression for the LDE.

precession minimum, regardless which orbital solution is chosen (supporting information Figures S9 and S10). This configuration, which also coincides with a maximum in the very long eccentricity cycle and a maximum in the 1.2 Myr obliquity cycle, leads to very warm summers in high northern latitudes because of the increased tilt of Earth's axis and perihelion occurring in Northern Hemisphere summer at maximum eccentricity. The calculation of the insolation curve is based on precession and obliquity, uncertainties in the orbital models for these parameters have repercussions on the insolation curve itself. These depend on the relative phase between precession and obliquity and on the effect caused by tidal dissipation. A change in these two parameters has implications on the amplitude and phase of the insolation curve (Lourens et al., 2004). However, a maximum in the very long eccentricity cycle and a maximum in the 1.2 Myr obliquity cycle occurring exactly at the same time will lead to exceptional insolation values in either Northern or Southern Hemisphere. Although we cannot determine from the current astronomical models in which hemisphere the maximum insolation occurs at 41.52 Ma, it is interesting that an experiment using a Global Climate Model with coupled terrestrial biosphere and soil components (e.g., DeConto et al., 2012, experiment 5) found that the combination of high eccentricity and high obliquity led to the release of more than 1,200 Pg C to the atmosphere causing a transient warming event. According to DeConto et al.'s (2012) model the insolation eventually reached a climatic threshold leading to permafrost thaw releasing the stored soil carbon. The existence and extent of permafrost areas in the Northern Hemisphere at 41 Ma is unknown. However, there is some indication that temperatures could have cooled enough (Stickley et al., 2009) to allow permafrost to form at high latitudes. If this scenario is considered, the question is why a hyperthermal event was not triggered already at 41.913 Ma ago when relatively high insolation values of $\sim 560 \text{ W m}^{-2}$ were reached. For answering this question it could be of major impor-

tance in which hemisphere the maximum insolation occurred, considering, for example, permafrost as a potential candidate for the initial warming.

Assuming that the cyclic variations in the carbon cycle as recorded in the changing $\delta^{13}\text{C}$ over hundreds of thousands and millions of years are driven by the expansion and contraction of biosphere productivity in response to changes in solar insolation (Pälike et al., 2006), the LLTM may have been caused by a significant biosphere productivity response to an extreme insolation event at 41.520 Ma. Strong variations in insolation on Milankovitch time scales will lead to a more extreme hydrological cycle. Thus, extremely high insolation values may have also led to a prolonged dry seasons which would reduce the accumulation of organic carbon and release carbon by oxidizing existing organic deposits (Zachos et al., 2010; Zeebe & Zachos, 2007). The astronomically extreme seasonal contrast may be amplified through feedback mechanisms releasing increasing amounts of terrestrial carbon (more CO_2 , enhanced warming and hydrological cycles) fueling the hyperthermal event (Kurtz et al., 2003). Warming of the deep sea would have fostered the release and diffusive loss of methane from clathrates acting as a positive feedback enhancing the initial warming pulse (Buffett & Archer, 2004). Coincidence of extreme insolation values and a hyperthermal event with 2°C warming in the deep sea suggest that the climate system has a thermal threshold as proposed in modeling studies (Lunt et al., 2011). The exceptional orbital forcing could have triggered a cascade of feedbacks (Bowen, 2013) leading to a short-lived global warming event as observed 41.52 Ma ago. Currently, it is difficult for any climate/carbon cycle model (including DeConto et al., 2012; Ridgwell & Schmidt, 2010; etc.) to explain the LLTM record and its relation to orbital forcing. To provide a much better understanding of the LLTM record, complex climate/carbon cycle models are needed that are able to simulate the proposed threshold behavior.

5. Conclusions

Up to now, the full magnitude of the LLTM and its global relevance have not been adequately characterized. The LLTM is of special interest because it coincides with the highest insolation value (573 W m^{-2}) of the last 45 Ma using the La2004 solution at 65°N on 21 June. Notably, an insolation value of $\sim 560 \text{ W m}^{-2}$ was reached about 400 kyr prior to the LLTM, but no CIE or peculiar Fe intensity peak point to a hyperthermal event at that time. The additional 13 W m^{-2} may have triggered a hyperthermal event. It would be of great interest for modeling studies to know the magnitude of the carbon and oxygen isotope excursion in the deep sea during the LLTM. The transient nature of the event makes it difficult to identify the LLTM in deep-sea sediments without high resolution (hundreds) of stable isotope analysis, but because of its position 72% up in chron C19r it should be feasible to locate the LLTM when a reliable magnetostratigraphy is available. More records from ocean basins other than the Atlantic are required to get a better handle on the global response of the CCD and on the true magnitude of the warming event.

Acknowledgments

We thank the Editor Adina Paytan, Ted Moore, and an anonymous referee for their helpful reviews and suggestions. We thank Henning Kuhnert and the stable isotope lab team at MARUM for analyses, Alex Wülbers and Walter Hale at the IODP Bremen Core Repository (BCR) for core handling, and Vera Lukies (MARUM) for assistance with XRF core scanning. This research used samples and data provided by the International Ocean Discovery Program (IODP). IODP is sponsored by the U.S. National Science Foundation (NSF) and participating countries. Financial support for this research was provided by the Deutsche Forschungsgemeinschaft (DFG). All data are open access available at <https://doi.pangaea.de/10.1594/PANGAEA.883619>. This research was supported by NSF award OCE16-58023 to R.E.Z.

References

- Anagnostou, E., John, E. H., Edgar, K. M., Foster, G. L., Ridgwell, A., Inglis, G. N., . . . Pearson, P. N. (2016). Changing atmospheric CO_2 concentration was the primary driver of early Cenozoic climate. *Nature*, *533*(7603), 380–384. <https://doi.org/10.1038/nature17423>
- Bohaty, S. M., Zachos, J. C., Florindo, F., & Delaney, M. L. (2009). Coupled greenhouse warming and deep-sea acidification in the middle Eocene. *Paleoceanography*, *24*, PA2207. <https://doi.org/10.1029/2008PA001676>
- Bornemann, A., Schulte, P., Sprong, J., Steurbaut, E., Youssef, M., & Speijer, R. P. (2009). Latest Danian carbon isotope anomaly and associated environmental change in the southern Tethys (Nile Basin, Egypt). *Journal of the Geological Society*, *166*(6), 1135–1142. <https://doi.org/10.1144/0016-76492008-104>
- Bowen, G. J. (2013). Up in smoke: A role for organic carbon feedbacks in Paleogene hyperthermals. *Global and Planetary Change*, *109*, 18–29. <https://doi.org/10.1016/j.gloplacha.2013.07.001>
- Buffett, B., & Archer, D. (2004). Global inventory of methane clathrate: Sensitivity to changes in the deep ocean. *Earth and Planetary Science Letters*, *227*(3–4), 185–199. <https://doi.org/10.1016/j.epsl.2004.09.005>
- Cande, S. C., & Kent, D. V. (1995). Revised calibration of the geomagnetic polarity timescale for the Late Cretaceous and Cenozoic. *Journal of Geophysical Research*, *100*(B4), 6093–6095. <https://doi.org/10.1029/94JB03098>
- Clement, B. M., & Hailwood, E. A. (1991). Magnetostratigraphy of sediments from Sites 701 and 702. In P. F. Ciesielski et al. (Eds.), *Proceedings of Ocean Drilling Program, scientific results* (Vol. 114, pp. 359–366). College Station, TX: Ocean Drilling Program. <https://doi.org/10.2973/odp.proc.sr.114.156.1991>
- Cramer, B. S., Wright, J. D., Kent, D. V., & Aubry, M.-P. (2003). Orbital climate forcing of $\delta^{13}\text{C}$ excursions in the late Paleocene-Eocene (chrons C24n-C25n). *Paleoceanography*, *18*(4), 1097. <https://doi.org/10.1029/2003PA000909>
- DeConto, R. M., Galeotti, S., Pagani, M., Tracy, D., Schaefer, K., Zhang, T., . . . Beerling, D. J. (2012). Past extreme warming events linked to massive carbon release from thawing permafrost. *Nature*, *484*(7392), 87–91. <https://doi.org/10.1038/nature10929>
- Dickens, G. R. (2003). Rethinking the global carbon cycle with a large, dynamic and microbially mediated gas hydrate capacitor. *Earth and Planetary Science Letters*, *213*(3–4), 169–183. [https://doi.org/10.1016/S0012-821X\(03\)00325-X](https://doi.org/10.1016/S0012-821X(03)00325-X)
- Dickens, G. R. (2011). Down the rabbit hole: Toward appropriate discussion of methane release from gas hydrate systems during the Paleocene-Eocene thermal maximum and other past hyperthermal events. *Climate of the Past*, *7*(3), 831–846. <https://doi.org/10.5194/cp-7-831-2011>
- Edgar, K. M., Wilson, P. A., Sexton, P. F., & Sugauma, Y. (2007). No extreme bipolar glaciation during the main Eocene calcite compensation shift. *Nature*, *448*(7156), 908–911. <https://doi.org/10.1038/nature06053>
- Erbacher, J., Mosher, D. C., & Malone, M. J. (2004). *Proceedings of Ocean Drilling Program, Initial Reports* (Vol. 207). College Station, TX: Ocean Drilling Program. <https://doi.org/10.2973/odp.proc.ir.207.2004>
- Erez, J., & Luz, B. (1983). Experimental paleotemperature equation for planktonic foraminifera. *Geochimica et Cosmochimica Acta*, *47*(6), 1025–1031. [https://doi.org/10.1016/0016-7037\(83\)90232-6](https://doi.org/10.1016/0016-7037(83)90232-6)
- Katz, M. E., & Miller, K. G. (1991). Early Paleogene benthic foraminiferal assemblage and stable isotopes in the Southern Ocean. In P. F. Ciesielski et al. (Eds.), *Proceedings of Ocean Drilling Program, scientific results* (Vol. 114, pp.49–96). College Station, TX: Ocean Drilling Program. <https://doi.org/10.2973/odp.proc.sr.114.147.1991>
- Kirtland Turner, S., Sexton, P. F., Charles, C. D., & Norris, R. D. (2014). Persistence of carbon release events through the peak of early Eocene global warmth. *Nature Geoscience*, *7*(10), 748–751. <https://doi.org/10.1038/ngeo2240>
- Kurtz, A. C., Kump, L. R., Arthur, M. A., Zachos, J. C., & Paytan, A. (2003). Early Cenozoic decoupling of the global carbon and sulfur cycles. *Paleoceanography*, *18*(4), 1090. <https://doi.org/10.1029/2003PA000908>
- Laskar, J., Robutel, P., Joutel, F., Gastineau, M., Correia, A., & Levrard, B. (2004). A long-term numerical solution for the insolation quantities of the Earth. *Astronomy and Astrophysics*, *428*(1), 261–285. <https://doi.org/10.1051/0004-6361:20041335>
- Lauretano, V., Hilgen, F. J., Zachos, J. C., & Lourens, L. J. (2016). Astronomically tuned age model for the early Eocene carbon isotope events: A new high-resolution $\delta^{13}\text{C}$ benthic record of ODP Site 1263 between ~ 49 and ~ 54 Ma. *Newsletters on Stratigraphy*, *49*(2), 383–400. <https://doi.org/10.1127/nos/2016/0077>
- Lauretano, V., Littler, K., Polling, M., Zachos, J. C., & Lourens, L. J. (2015). Frequency, magnitude and character of hyperthermal events at the onset of the Early Eocene Climatic Optimum. *Climate of the Past*, *11*(10), 1313–1324. <https://doi.org/10.5194/cp-11-1313-2015>
- Leon-Rodríguez, L., & Dickens, G. R. (2010). Constraints on ocean acidification associated with rapid and massive carbon injections: The early Paleogene record at ocean drilling program site 1215, equatorial Pacific Ocean. *Paleogeography, Palaeoclimatology, Palaeoecology*, *298*(3–4), 409–420. <https://doi.org/10.1016/j.palaeo.2010.10.029>
- Lourens, L. J., Hilgen, F. J., Laskar, J., Shackleton, N. J., & Wilson, D. (2004). The Neogene period. In F. Gradstein, J. Ogg, & A. Smith (Eds.), *A geological timescale 2004* (pp. 409–440). Cambridge, UK: Cambridge University Press. <https://doi.org/10.1017/CBO9780511536045.022>
- Lourens, L. J., Sluijs, A., Kroon, D., Zachos, J. C., Thomas, E., Röhl, U., . . . Raffi, I. (2005). Astronomical pacing of late Palaeocene to early Eocene global warming events. *Nature*, *435*(7045), 1083–1087. <https://doi.org/10.1038/nature03814>

- Lunt, D. J., Ridgwell, A., Sluijs, A., Zachos, J., Hunter, S., & Haywood, A. (2011). A model for orbital pacing of methane hydrate destabilization during the Palaeogene. *Nature Geoscience*, 4(11), 775–778. <https://doi.org/10.1038/ngeo1266>
- Nicolo, M. J., Dickens, G. R., Hollis, C. J., & Zachos, J. C. (2007). Multiple early Eocene hyperthermals: Their sedimentary expression on the New Zealand continental margin and in the deep sea. *Geology*, 35(8), 699–702. <https://doi.org/10.1130/G23648A.1>
- Ogg, J. G., & Bardot, L. (2001). Aptian through Eocene magnetostratigraphic correlation of the Blake Nose Transect (Leg 171B), Florida Continental Margin. In D. Kroon, R. D. Norris, & A. Klaus (Eds.), *Proceedings of Ocean Drilling Program, scientific results* (Vol. 171B, pp. 1–58). College Station, TX: Ocean Drilling Program. <https://doi.org/10.2973/odp.proc.sr.171b.104.2001>
- Pagani, M., Caldeira, K., Archer, D., & Zachos, J. C. (2006). An ancient carbon mystery. *Science*, 314(5805), 1556–1557. <https://doi.org/10.1126/science.1136110>
- PALAEOSSENS Project Members. (2012). Making sense of palaeoclimate sensitivity. *Nature*, 491(7426), 683–691. <https://doi.org/10.1038/nature11574>
- Pälike, H., Norris, R. D., Herrle, J. O., Wilson, P. A., Coxall, H. K., Lear, C. H., . . . Wade, B. S. (2006). The heartbeat of the Oligocene climate system. *Science*, 314(5807), 1894–1898. <https://doi.org/10.1126/science.1133822>
- Penman, D. E., Turner, S. K., Sexton, P. F., Norris, R. D., Dickens, A. J., Bouliia, S., . . . Röhl, U. (2016). An abyssal carbonate compensation depth overshoot in the aftermath of the Palaeocene-Eocene Thermal Maximum. *Nature Geoscience*, 9(8), 575–580. <https://doi.org/10.1038/ngeo2757>
- Ridgwell, A., & Schmidt, D. N. (2010). Past constraints on the vulnerability of marine calcifiers to massive carbon dioxide release. *Nature Geoscience*, 3, 196–200. <https://doi.org/10.1038/ngeo755>
- Sexton, P. F., Norris, R. D., Wilson, P. A., Pälike, H., Westerhold, T., Röhl, U., . . . Gibbs, S. (2011). Eocene global warming events driven by ventilation of oceanic dissolved organic carbon. *Nature*, 471(7338), 349–352. <https://doi.org/10.1038/nature09826>
- Sexton, P. F., Wilson, P. A., & Norris, R. D. (2006). Testing the Cenozoic multisite composite $\delta^{18}\text{O}$ and $\delta^{13}\text{C}$ curves: New monospecific Eocene records from a single locality, Demerara Rise (Ocean Drilling Program Leg 207). *Paleoceanography*, 21(2), PA2019. <https://doi.org/10.1029/2005PA001253>
- Shipboard Scientific Party. (1988). Site 702. In P. F. Ciesielski et al. (Eds.), *Proceedings of Ocean Drilling Program, initial reports* (Vol. 114, pp. 483–548). College Station, TX: Ocean Drilling Program. <https://doi.org/10.2973/odp.proc.ir.114.109.1988>
- Stap, L., Lourens, L. J., Thomas, E., Sluijs, A., Bohaty, S., & Zachos, J. C. (2010). High-resolution deep-sea carbon and oxygen isotope records of Eocene Thermal Maximum 2 and H2. *Geology*, 38(7), 607–610. <https://doi.org/10.1130/g30777.1>
- Stickley, C. E., St John, K., Koc, N., Jordan, R. W., Passchier, S., Pearce, R. B., & Kearns, L. E. (2009). Evidence for middle Eocene Arctic sea ice from diatoms and ice-rafted debris. *Nature*, 460(7253), 376–379. <https://doi.org/10.1038/nature08163>
- Van Andel, T. H. (1975). Mesozoic/cenozoic calcite compensation depth and the global distribution of calcareous sediments. *Earth and Planetary Science Letters*, 26(2), 187–194. [https://doi.org/10.1016/0012-821x\(75\)90086-2](https://doi.org/10.1016/0012-821x(75)90086-2)
- Vandenbergh, N., Hilgen, F. J., Speijer, R. P., Ogg, J. G., Gradstein, F. M., Hammer, O., . . . Hooker, J. J. (2012). Chapter 28—The Paleogene period. In F. M. Gradstein, J. G. Ogg, M. D. Schmitz, & G. M. Ogg (Eds.), *The geologic time scale* (pp. 855–921). Boston, MA: Elsevier. <https://doi.org/10.1016/B978-0-444-59425-9.00028-7>
- Westerhold, T., & Röhl, U. (2013). Orbital pacing of Eocene climate during the Middle Eocene climate optimum and the chron C19r event: Missing link found in the tropical western Atlantic. *Geochemistry, Geophysics, Geosystems*, 14, 4811–4825. <https://doi.org/10.1002/ggge.20293>
- Westerhold, T., Röhl, U., Frederichs, T., Agnini, C., Raffi, I., Zachos, J. C., & Wilkens, R. H. (2017). Astronomical calibration of the Ypresian time-scale: Implications for seafloor spreading rates and the chaotic behavior of the solar system? *Climate of the Past*, 13(9), 1129–1152. <https://doi.org/10.5194/cp-13-1129-2017>
- Westerhold, T., Röhl, U., Frederichs, T., Bohaty, S. M., & Zachos, J. C. (2015). Astronomical calibration of the geological timescale: Closing the middle Eocene gap. *Climate of the Past*, 11(9), 1181–1195. <https://doi.org/10.5194/cp-11-1181-2015>
- Westerhold, T., Röhl, U., Donner, B., McCarren, H. K., & Zachos, J. C. (2011). A complete high-resolution Paleocene benthic stable isotope record for the central Pacific (ODP Site 1209). *Paleoceanography*, 26, PA2216. <https://doi.org/10.1029/2010PA002092>
- Zachos, J. C., Dickens, G. R., & Zeebe, R. E. (2008). An early Cenozoic perspective on greenhouse warming and carbon-cycle dynamics. *Nature*, 451(7176), 279–283. <https://doi.org/10.1038/nature06588>
- Zachos, J. C., Kroon, D., Blum, P., et al. (2004). *Proceedings of Ocean Drilling Program, initial reports* (Vol. 208). College Station, TX: Ocean Drilling Program. <https://doi.org/10.2973/odp.proc.ir.208.2004>
- Zachos, J. C., McCarren, H., Murphy, B., Röhl, U., & Westerhold, T. (2010). Tempo and scale of late Paleocene and early Eocene carbon isotope cycles: Implications for the origin of hyperthermals. *Earth and Planetary Science Letters*, 299(1–2), 242–249. <https://doi.org/10.1016/j.epsl.2010.09.004>
- Zachos, J. C., Pagani, M., Sloan, L., Thomas, E., & Billups, K. (2001). Trends, rhythms, and aberrations in global climate 65 Ma to present. *Science*, 292(5517), 686–693. <https://doi.org/10.1126/science.1059412>
- Zachos, J. C., Röhl, U., Schellenberg, S. A., Sluijs, A., Hodel, D. A., Kelly, D. C., . . . Kroon, D. (2005). Rapid acidification of the ocean during the Paleocene-Eocene thermal maximum. *Science*, 308(5728), 1611–1615. <https://doi.org/10.1126/science.1109004>
- Zeebe, R. E. (2012). LOSCAR: Long-term ocean-atmosphere-sediment carbon cycle reservoir model v2.0.4. *Geoscientific Model Development*, 5(1), 149–166.
- Zeebe, R. E., & Zachos, J. C. (2007). Reversed deep-sea carbonate ion basin gradient during Paleocene-Eocene thermal maximum. *Paleoceanography*, 22, PA3201. <https://doi.org/10.1029/2006PA001395>